A Novel Class of Clathrin-coated Vesicles Budding from Endosomes

Willem Stoorvogel, Viola Oorschot, and Hans J. Geuze

Department of Cell Biology, Faculty of Medicine, Institute of Biomembranes, Utrecht Universiteit, The Netherlands

Abstract. Clathrin-coated vesicles transport selective integral membrane proteins from the plasma membrane to endosomes and from the TGN to endosomes. Recycling of proteins from endosomes to the plasma membrane occurs via unidentified vesicles. To study this pathway, we used a novel technique that allows for the immunoelectron microscopic examination of transferrin receptor–containing endosomes in nonsectioned cells. Endosomes were identified as separate discontinuous tubular-vesicular entities. Each endosome was decorated, mainly on the tubules, with many clathrin-coated buds. Endosome-associated clathrin-coated buds were discerned from plasma membrane–derived clathrin-coated vesicles by three criteria: size (60 nm and 100 nm, respectively), continuity with endosomes, and the lack of labeling for α-adaptin. They were also distinguished from TGN-derived clathrin-coated vesicles by their location at the periphery of the cell, size, and the lack of labeling for γ-adaptin. In the presence of brefeldin A, a large continuous endosomal network was formed. Transferrin receptor recycling as well as the formation of clathrin-coated pits at endosomes was inhibited in the presence of brefeldin A. Together with the localization of transferrin receptors at endosome-associated buds, this indicates that a novel class of clathrin-coated vesicles serves an exit pathway from endosomes. The target organelles for endosome-derived clathrin-coated vesicles remain, however, to be identified.

CELLS accomplish selective removal of integral membrane proteins from the plasma membrane by endocytosis. Endocytosis includes the formation of clathrin-coated vesicles that bud off from the plasma membrane into the cell. After uncoating, these vesicles fuse with sorting endosomes that are localized throughout the cytoplasma. In sorting endosomes, composed of vacuoles with attached tubular extensions (Geuze et al., 1983; Hopkins et al., 1990), proteins are sorted and transported to different destinations. Soluble molecules, ligands that dissociate from their receptors in endosomes and fluid phase–endocytosed material, are largely transported from sorting endosomes to lysosomes. In contrast, most endocytosed integral membrane proteins recycle efficiently to the plasma membrane, probably via the tubular endosomal extensions (Geuze et al., 1983, 1987; Courtoy et al., 1991; Trowbridge et al., 1993), either directly or via perinuclear recycling endosomes (Ghosh and Maxfield, 1995). However, many endocytosed membrane proteins are not efficiently recycled to the plasma membrane. Examples are the cation-independent mannose 6-phosphate receptor (MPR)[1] (Stoorvogel et al., 1989; Riederer et al., 1994) and TGN38 (Wong and Hong, 1993) that are transported to the TGN, and lysosomal glycoproteins (for review see Fukuda, 1991; Guarnieri et al., 1993) and the EGF receptor (Felder et al., 1990; Futter et al., 1993) that can be transported to lysosomes. Transport from sorting endosomes to the TGN (Geuze and Morré, 1991) and the plasma membrane may occur via recycling endosomes (Ghosh and Maxfield, 1995; Hopkins et al., 1994).

The molecular machinery responsible for active sorting of integral membrane proteins in sorting endosomes has so far not been identified (Trowbridge et al., 1993; Luzio and Banting, 1993; Sandoval and Bakke, 1994). Endosome-derived vesicles serving exit pathways have also not been identified. Such vesicles can be expected to display cytoplasmic coats analogous to the four types of coated transport vesicles identified for other pathways: COP I- and COP II-coated vesicles, budding from Golgi cisternae (for review see Rothman, 1994) and the ER (Barlowe et al., 1994), respectively, and two types of clathrin-coated vesicles, formed at the plasma membrane and the TGN (for reviews see Keen, 1990; Robinson, 1994). Clathrin-coated vesicles are intermediates in the transport pathways from the plasma membrane to endosomes and from the TGN to endosomes. Specific sets of integral membrane proteins are incorporated in clathrin-coated vesicles through binding to cytosolic adaptor complexes, AP1 at the TGN and AP2 at the plasma membrane (Pearse and Robinson, 1990; Robinson, 1994). The fungal metabolite brefeldin A (BFA) aided in the elucidation of the role of coat proteins in vesicular

Address all correspondence to W. Stoorvogel, Laboratory of Cell Biology, Utrecht University, AZU Heidelberglaan 100, Room H02.314, 3584 CX Utrecht, The Netherlands. Tel.: (31)-30-2506551 or 2507577. Fax: (31)-30-2541797.

1. *Abbreviations used in this paper*: BFA, brefeldin A; MPR, cation-independent mannose 6-phosphate receptor; TfR, transferrin receptor.

transport. Originally, BFA has been acknowledged to cause the formation of long tubular extensions from the Golgi apparatus and to induce a redistribution of Golgi components to the ER (Fujiwara et al., 1988; Lippincott-Schwartz et al., 1989; Doms et al., 1989). BFA also induces the formation of long membranous tubules at the TGN and at endosomes (Lippincott-Schwartz et al., 1991; Wood et al., 1991; Hunziger et al., 1991). BFA exerts its effect by preventing binding of ARF as well as AP1 and β-COP to the TGN and *cis*-Golgi, respectively (Randazzo et al., 1993, and references therein). The identical effect of BFA on the Golgi, TGN, and endosomes with respect to the induction of long tubules suggests the presence of yet unidentified, BFA-sensitive, coat proteins on endosomes. Such coats may be instrumental for selective and efficient recycling of integral membrane proteins from sorting endosomes to the plasma membrane, and/or for transport from endosomes to the TGN.

The endocytic pathway is composed of a vacuolar system that is very heterogeneous in morphology, protein composition, and subcellular distribution. To study exit pathways from endosomes at the ultrastructural level, we developed a novel technique that allows visualization and immunolabeling of the endocytic system in nonsectioned cells at the electron microscopic level. We show that endosomes do not form a continuous membranous tubular network. Instead, transferrin receptor (TfR)–containing clathrin-coated buds continuous with endosomal vacuoles and tubules were found. These endosome-associated clathrin-coated buds are distinct from plasma membrane– and TGN-derived clathrin-coated vesicles. In conclusion, clathrin-coated vesicles provide for an exit pathway from endosomes, via which recycling to the plasma membrane may occur.

Materials and Methods

Cell Culture

A431 cells were cultured in high glucose DME supplemented with 10% FCS, penicillin, and streptomycin according to standard procedures. For whole-mount immunocytochemistry, cells were grown on golden grids carrying a carbon-coated Formvar film. The grids were incubated for 1 d in culture medium before cell seeding. Cells cultured on grids were used for experiments after 2 d of culturing.

Endocytosis of Tf/HRP

The Tf/HRP conjugate was prepared and analyzed as described (Stoorvogel et al., 1988). The conjugate bound specifically and in a saturable manner to the TfR, its recycling kinetics were identical to that of nonconjugated Tf, and Tf/HRP was retrieved as a complex in the culture medium after cycling through the cell (Stoorvogel et al., 1988). After 1 h of continuous uptake, no Tf/HRP was mistargeted to lysosomes as determined by cell fractionation on Percoll density gradients (not shown).

To label the entire TfR pathway, cells were first washed with MEM, containing 20 mM Hepes/NaOH, pH 7.2, lacking bicarbonate (MEMH), and then incubated for 1 h at 37°C in MEMH containing 25 μg/ml Tf/HRP. When indicated, the medium was supplemented with 10 μg/ml BFA for the last 1–30 min of incubation. For plasma membrane labeling, washed cells were first incubated for 30 min in MEMH at 37°C and then incubated for 1 h in MEMH containing 25 μg/ml Tf/HRP at 0°C. After endocytic uptake or binding of Tf/HRP, the medium was removed and replaced immediately by MEMH at 0°C. The cells were washed twice with MEMH at 0°C (~5 s per wash) and incubated for 30 min at 0°C in freshly prepared DAB buffer. DAB buffer contained 1.5 mg/ml DAB (BDH Chemicals Ltd., Poole, UK), 70 mM NaCl, 50 mM ascorbic acid (Merck, Darmstadt, Germany), 20 mM Hepes (Gibco BRL, Uxbridge, UK), and was adjusted to pH 7.0 using 5 N NaOH. After setting the pH, the solution was adjusted to 300 mosM using NaCl. The DAB buffer was supplemented with 0.02% H_2O_2 just before use. When indicated, ascorbic acid was omitted from the DAB buffer to allow extracellular HRP-mediated DAB polymerization. Additional NaCl was added to this buffer to compensate the loss in osmolarity.

Preparing Cells for Immunocytochemistry

After the HRP-mediated polymerization of DAB in endocytic compartments, cells were washed three times with PBS (Dulbecco's PBS lacking $CaCl_2$ and $MgCl_2$) at 0°C. Soluble cytosolic proteins were removed by permeabilizing the cells in PBS, 1 mM EGTA, 0.5 mM $MgCl_2$, 0.5 mg/ml saponin (Merck) at 0°C. Saponin binds to cholesterol in membranes, forming pores through which soluble cytosolic proteins leak out. Membrane-bound proteins, the nucleus, cytoskeleton, and proteins cross-linked to the DAB polymer remained cell associated (Rijnboutt et al., 1991). After 30 min the cells were washed three times with PBS, 1 mM EGTA, 0.5 mM $MgCl_2$, and fixed for 1 h at 4°C with 1% paraformaldehyde in PBS. When indicated, clathrin and adaptor complexes were removed from membranes before the paraformaldehyde fixation. Towards this goal, saponin-washed cells were incubated for 15 min at 0°C in 0.5 M Tris/HCl, pH 7.4 (Mahaffey et al., 1990). Tris was removed by extensive washing with PBS before fixation. All the following treatments were performed at room temperature. The cells were washed three times with PBS after which free reactive aldehyde groups were blocked during a 5-min incubation in PBS, 20 mM glycine. The grids were transferred to blocking buffer (PBS, 0.5 mg/ml saponin, 20 mM glycine, 0.1% cold water fish gelatin [Sigma Chemical Co., St. Louis, MO; G-7765], 0.02% NaN_2). The cells were immuno–double-labeled (Slot et al., 1991) using 5-nm and 10-nm protein A–colloidal gold particles. The cells were fixed with glutaraldehyde after each of the sequential labeling steps to permanently immobilize the colloidal gold label and to exclude cross-labeling (Slot et al., 1991). Cross-labeling was checked in control experiments in which the primary antibody of the second label was omitted and found negligible. Nonspecific labeling was checked using nonrelevant antibodies. The cytoplasmic tail of the TfR was labeled using mAb HTR-H68.4 (Schmid and Smythe, 1991) which was prepared and provided generously by Dr. Trowbridge (Salk Institute, La Jolla, CA). Monoclonal mouse anti-γ-adaptin, 100/3 (Ahle et al., 1988), and polyclonal rabbit anticlathrin light chain were gifts from Dr. Ungewickell (Washington University, St. Louis, MO). Another polyclonal antibody directed against clathrin light chain was obtained from Dr. Keen (Thomas Jefferson University, Philadelphia, PA). The mAbs directed against clathrin light chain, CON.1 (Näthke et al., 1992), clathrin heavy chain, X22 (Brodsky, 1985), and α-adaptin, AP.6 (Chin et al., 1989) were kindly provided by Dr. Brodsky (University of California, San Francisco). Polyclonal anticlathrin heavy chain was a gift from Dr. Robinson (Cambridge University, Cambridge, UK). Detection of all monoclonal antibodies was performed using rabbit anti–mouse Ig (Dakopatts, Copenhagen, Denmark).

After immunolabeling and fixation, the cells were extensively washed with H_2O, and dehydrated by sequential passage through 50, 70, 90, 96%, and absolute ethanol. The ethanol was substituted by liquid CO_2, and the samples were dried using a critical point–drying apparatus. Finally, a film of evaporated carbon was applied on the samples while rotating the grids under varying angles. The grids were examined using a transmission electron microscope (Jeol USA, Peabody, MA) at 60–80 kV.

Cell surface ^{125}I Labeling, Immunoprecipitation, and SDS-PAGE

Cells, cultured on 6-cm dishes, were washed three times with MEMH and incubated for 60 min in MEMH at 37°C in a water bath to remove serum Tf. Next, the cell surface was ^{125}I labeled as described previously (Stoorvogel et al., 1989). Endocytosis of surface ^{125}I-labeled proteins was allowed for 30 min at 37°C in MEMH containing 25 μg/ml Tf/HRP. Endocytosis was stopped and excess Tf/HRP removed by washing the cells three times with PBS, 1 mM EDTA at 0°C. When indicated, the cells were incubated for 1 h in 1 ml PBS, 1 mM EDTA, 0.5 mg/ml proteinase K at 0°C on a rocker platform to digest plasma membrane proteins. The protease activity was stopped by the addition of 1 mM PMSF. The detached cells were collected and washed twice with PBS, 1 mM EDTA, 1 mM PMSF by centrifugation for 5 min at 300 *g* at 0°C. Samples of the cell suspension were incubated in DAB buffer as described above. After the DAB cytochemistry, the cells were washed twice with PBS, 1 mM EDTA, 1 mM PMSF by centrifuga-

tion for 5 min at 300 *g* and lysed for 10 min at 0°C in 0.5 ml PBS, 1% Triton X-100, 0.1% SDS, 1 mM PMSF, 0.02% NaN_3, 1 mM EDTA. Nuclei were removed from the lysate by centrifugation for 1 min at 10,000 *g*, and TfR was immunoprecipitated according to standard procedures (Stoorvogel et al., 1989). ^{125}I-TfR was analyzed by SDS-PAGE, and visualized and quantified using a Phosphor Imager (Molecular Dynamics, Sunnyvale, CA).

Results

Endosomes were studied using a novel technique that allows for the visualization of endosomes in nonsectioned cells by transmission electron microscopy. Toward this purpose cells were cultured on Formvar-coated grids. The endocytic pathway traveled by the TfR was labeled with Tf/HRP during a 60-min incubation at 37°C. After Tf/HRP uptake the cells were placed at 0°C in a buffer containing DAB, H_2O_2, and ascorbic acid. Monomeric DAB easily penetrates nonfixed membranes, but is captured after HRP-catalyzed polymerization (Courtoy et al., 1984). Ascorbic acid, a membrane-impermeable antioxidant, inhibited Tf/HRP-catalyzed DAB polymerization at the plasma membrane but not in endosomes. DAB polymerization in endosomes resulted in three advantageous effects: (i) Electron-dense DAB polymer served as an endosomal marker that was easily detected using electron microscopy. (ii) The endosomal protein content, including integral membrane proteins, was cross-linked to the DAB polymer, resulting in the selective fixation of the endosomal structure. Nonendosomal proteins were not fixed. Consequently, cytosolic proteins could be removed after permeabilizing the cells with saponin. The resulting electron-lucent cells could then be studied, as whole-mount preparations, using transmission electron microscopy. (iii) Efficient removal of cytosol assured maximal accessibility of epitopes at the cytoplasmic surface of endosomes. Together with the whole-mount aspect, this resulted in very high labeling efficiencies.

Both endosomes and the plasma membrane were labeled with peroxidase activity when cells were incubated at 37°C in the presence of Tf/HRP. A subsequent incubation in the presence of DAB and H_2O_2 resulted in the HRP-catalyzed deposition of DAB polymer at these two locations. For our whole-mount immunoelectron microscopical studies it was essential to prevent DAB polymerization at the plasma membrane. To study DAB polymerization at the plasma membrane (Fig. 1 *A*), the surface of A431 cells was ^{125}I labeled, and Tf/HRP was bound to plasma membrane TfRs at 0°C. The cells were then incubated in the presence of DAB and H_2O_2, washed, and lysed. As a consequence of the peroxidation reaction, membrane proteins were encapsulated by DAB polymer rendering them detergent insoluble. Analysis by SDS-PAGE revealed large ^{125}I-labeled protein complexes that failed to migrate into the stacking gel (Fig. 1 *A*, lane *1*). The addition of ascorbic acid to the DAB solution prevented the formation of ^{125}I-labeled protein aggregates (Fig. 1 *A*, lane *2*), and the formation of a DAB precipitate on these cells was not detected (not shown). We conclude that during the peroxidation reaction, ascorbic acid competed with DAB as reductant, yielding oxidized ascorbic acid, a soluble reaction product. Previously, we have reported that proteins present in HRP-containing endosomes became cross-linked to DAB polymer upon incubation of intact cells in the presence of DAB and H_2O_2 (Stoorvogel et al., 1991*a*; Rijnboutt et al., 1992; Strous et al., 1993). Consistent with this we found cross-linked ^{125}I-labeled proteins after allowing uptake of endocytosing surface ^{125}I-labeled proteins in the presence of Tf/HRP. The extracellular presence of ascorbic acid did not prevent cross-linking of endocytosed ^{125}I-labeled proteins by endocytosed Tf/HRP, as evidenced by ^{125}I-labeled aggregates recovered on top of the stacking gel (Fig. 1 *A*, lane *3*). Some of the ^{125}I-labeled proteins were lost during the incubation at 37°C, probably because they represent adhering serum proteins that dissociated from the culture dish at 37°C (not shown).

The TfR was used as a model protein to show that endocytosed proteins were efficiently cross-linked and that the extracellular presence of ascorbic acid did not interfere with this process (Fig. 1 *B*). Surface ^{125}I-labeled TfR was immunoprecipitated from a detergent extract and analyzed by SDS-PAGE (Fig. 1 *B*, lane *1*). A treatment of intact ^{125}I-labeled cells with proteinase K at 0°C completely removed all surface ^{125}I-TfR (Fig. 1 *B*, lane *2*). After endocytosis at 37°C in the presence of Tf/HRP, cell surface

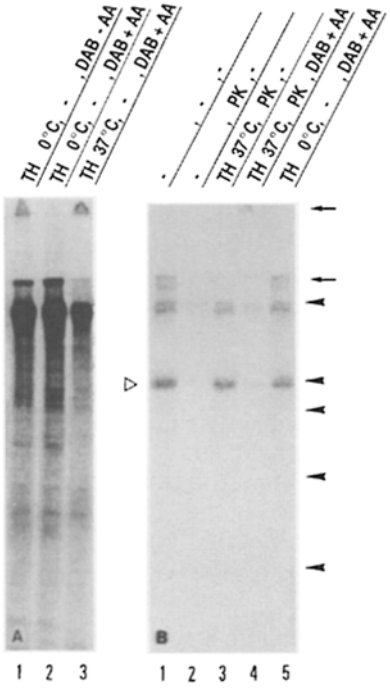

Figure 1. Selective DAB polymerization in endosomes. Cell surface proteins were ^{125}I labeled at 0°C. Samples of total cell lysates (*A*) or immunoprecipitated ^{125}I-TfR (*B*) were analyzed by SDS-PAGE and autoradiography. ^{125}I-labeled cells were incubated in the presence of Tf/HRP (*TH*) at 0°C (*A*, lanes *1* and *2*; *B*, lane *5*) or 37°C (*A*, lane *3*; *B*, lanes *3* and *4*) or in the absence of Tf/HRP at 0°C (*B*, lanes *1* and *2*). Some of the culture dishes were then incubated with proteinase K (*PK*) at 0°C to remove TfR at the plasma membrane (*B*, lanes *2–4*). Next, some cell cultures were incubated in the presence of DAB and H_2O_2 only (*A*, lane *1*), or in the presence of DAB, H_2O_2, and ascorbic acid (*AA*) (*A*, lanes *2* and *3*; *B*, lanes *4* and *5*). ^{125}I-TfR is indicated with an open triangle. Some nonreduced dimeric ^{125}I-TfR is found just below the 200-kD marker. Molecular mass (200, 92, 69, 46, and 30 kD) is indicated at the right (*arrowheads*). Top of the running and stacking gel is indicated with arrows at the right.

^{125}I-TfR was removed by the proteinase K treatment leaving only internalized ^{125}I-TfR intact (Fig. 1 *B*, lane *3*). When similarly treated cells were additionally incubated in the presence of DAB, H_2O_2, and ascorbic acid, endocytosed ^{125}I-TfR was cross-linked to DAB polymer with an efficiency of 85% (Fig. 1 *B*, lane *4*). Of the ^{125}I-labeled cross-linked endosomal protein complex, only a small proportion could be immunoprecipitated using anti-TfR antibodies, possibly due to epitope masking by DAB polymer, and was recovered as a complex on top of the stacking gel. In contrast to endosomal ^{125}I-TfR, ^{125}I-TfR at the plasma membrane was not cross-linked in the presence of ascorbic acid (Fig. 1 *B*, lane *5*). Thus, ascorbic acid is a membrane-impermeable reducing agent that competed extracellularly, but not intracellularly, with DAB as a substrate for HRP.

Next, we studied Tf/HRP-mediated DAB polymerization at the plasma membrane and in endosomes using whole-mount electron microscopy. TfRs at the plasma membrane were allowed to bind Tf/HRP at 0°C, after which the cells were incubated with DAB/H_2O_2 either in the absence or presence of ascorbic acid. After DAB polymerization the cells were washed in the presence of saponin resulting in membrane permeabilization. Consequently, soluble proteins from the cytosol and intracellular vacuoles leaked out of the cells (Rijnboutt et al., 1991) while membrane-associated proteins and proteins that were cross-linked to the DAB polymer remained cell associated. Although saponin-induced pores have a reported diameter of 8 nm (Dourmashkin et al., 1962), they allowed passage of protein A complexed to 5 nm and 10 nm colloidal gold. Upon saponin removal, permeabilization for protein A–colloidal gold complexes was reversed (not shown), indicating maintenance of the integrity of the plasma membrane. Due to the saponin treatment the cells became electron lucent, allowing visualization of electron-dense DAB polymer. After the saponin treatment the cells were fixed with paraformaldehyde and immunolabeled. DAB polymer was detected at sites with a diameter of 100 nm which labeled for both clathrin (10 nm gold) and α-adaptin (5 nm gold), identifying them as plasma membrane–associated clathrin-coated pits (Fig. 2). When ascorbic acid was present during the DAB reaction, sites labeled for clathrin and α-adaptin were negative for DAB polymer (not shown). Consequently, DAB staining in the presence of ascorbic acid, detected after endocytic uptake of Tf/HRP, must be attributed to endosome labeling.

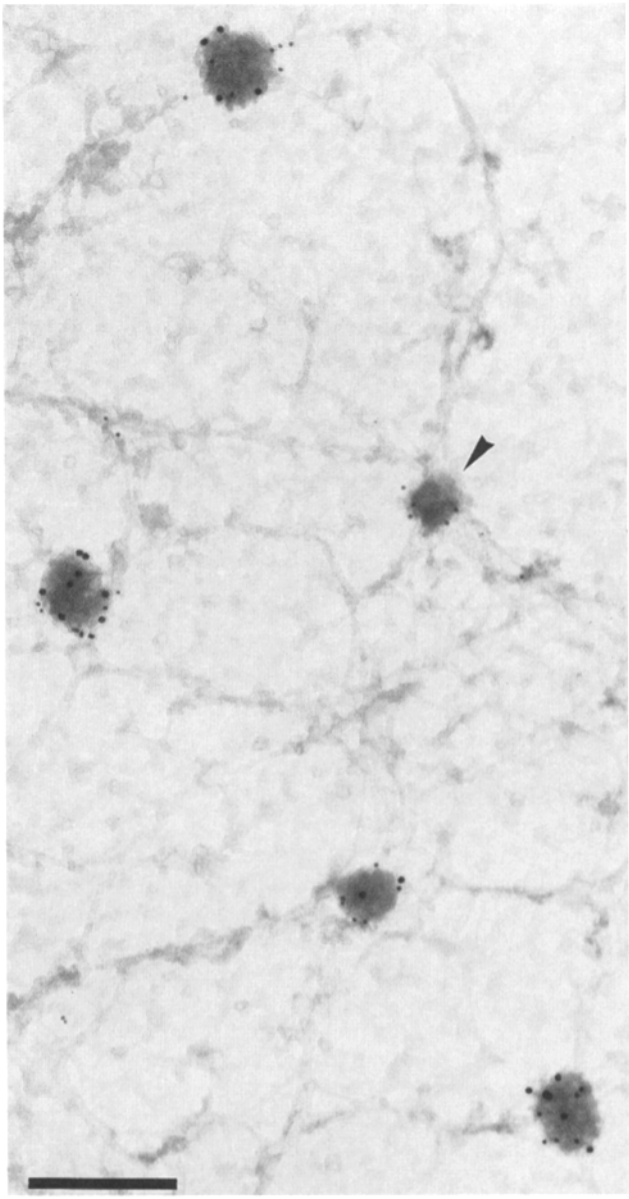

Figure 2. Plasma membrane–associated clathrin-coated pits. Cells were allowed to bind Tf/HRP for 60 min at 0°C. After removal of nonbound Tf/HRP, the cells were incubated at 0°C in the presence of DAB and H_2O_2. After removal of soluble cytosolic proteins in the presence of saponin, the cells were processed for whole-mount immunoelectron microscopy. The cells were labeled with protein A complexed to 5-nm and 10-nm gold particles for the demonstration of α-adaptin (AP.6) and clathrin light chain (polyclonal Ungewickell), respectively. DAB polymer and α-adaptin were found at clathrin-coated pits. One DAB-stained profile is labeled for α-adaptin only (*arrowhead*). Bar, 0.2 μm.

Endosomes Form a Continuous Tubular Network in the Presence of BFA But Not at Control Conditions

Although endosomal tubules may have a considerable length (Hopkins et al., 1990; Tooze and Hollinshead, 1991), it is not clear whether individual endosomes are connected with each other via a continuous membranous tubular network. However, it has been widely accepted that endosomes form a large tubular network in the presence of BFA (Lippincott-Schwartz et al., 1991; Wood et al., 1991; Hunziger et al., 1991). To address questions on the extent of the endosomal tubular network in the absence of BFA, it had to be verified that the experimental conditions used to prepare the whole-mount preparations did not interfere with the continuity of endosomal tubules. To validate the

Figure 3. Endosomes form a tubular network in the presence but not in the absence of BFA. Cells were allowed to endocytose Tf/HRP for 60 min at 37°C. BFA was either absent (*A* and *B*) or present during the last 5 min of this incubation (*C*). Then the cells were incubated at 0°C in the presence of H_2O_2, DAB, and ascorbic acid. Soluble cytosolic proteins were removed by washing in the presence of

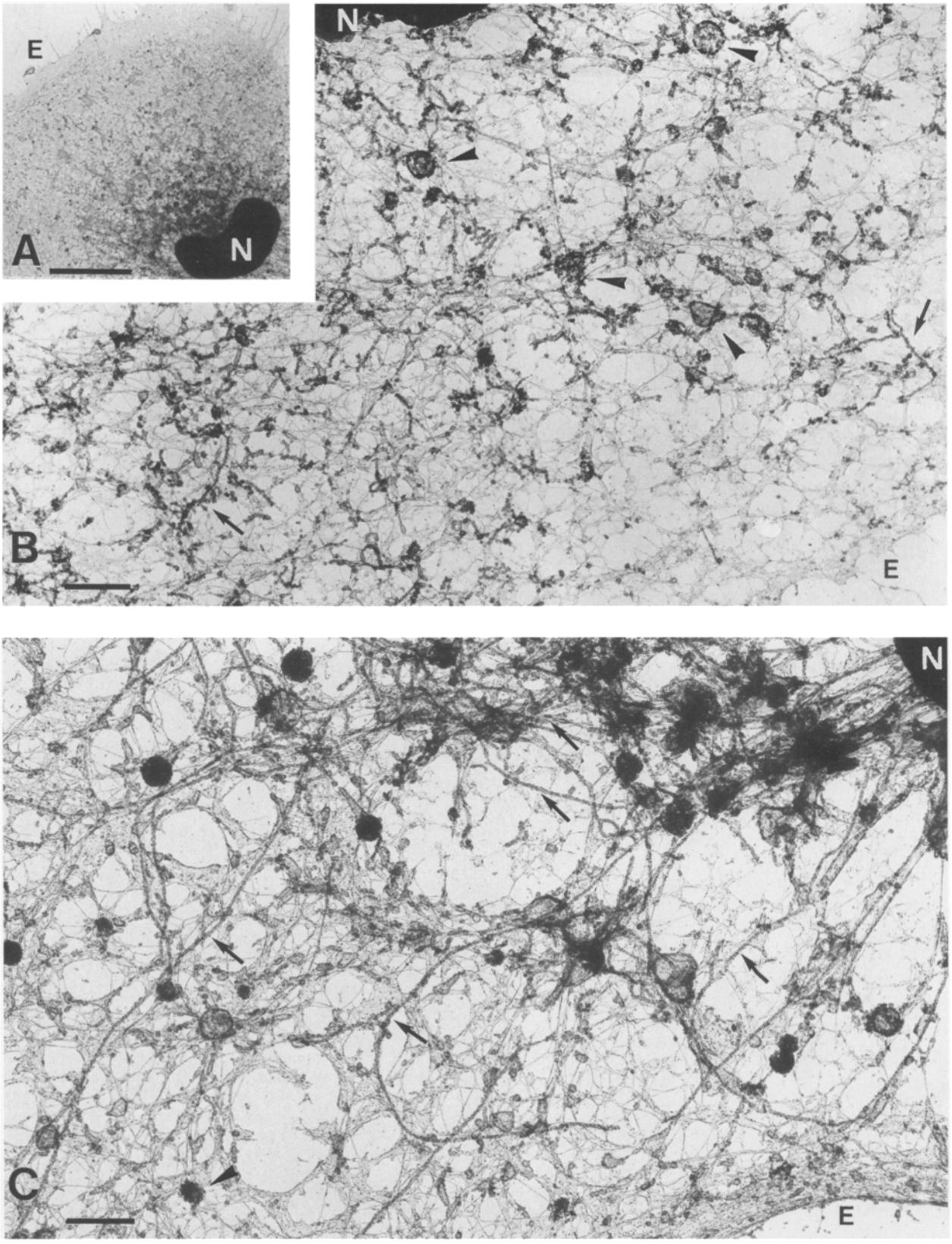

saponin, and the cells were processed for whole-mount electron microscopy. The nucleus (*N*) and the edge of the cells (*E*) are indicated. (*A*) a low magnification of cell showing perinuclear and peripheral DAB staining. Bar, 10 μm. (*B*) Numerous individual endosomes consisting of vacuoles (*arrowheads*) and tubules of sometimes considerable length (*arrows*) are identified by the electron-dense DAB precipitate. Nonidentified, less electron-dense meshworks, probably representing cytoskeleton, are also visualized. Bar, 1 μm. (*C*) A BFA-treated cell shows a continuous tubular network (*arrows*) ranging from the periphery to the perinuclear area of the cell. Endosomal vacuoles, often discontinuous with the tubular network (*arrowhead*) were also encountered. Bar, 1 μm.

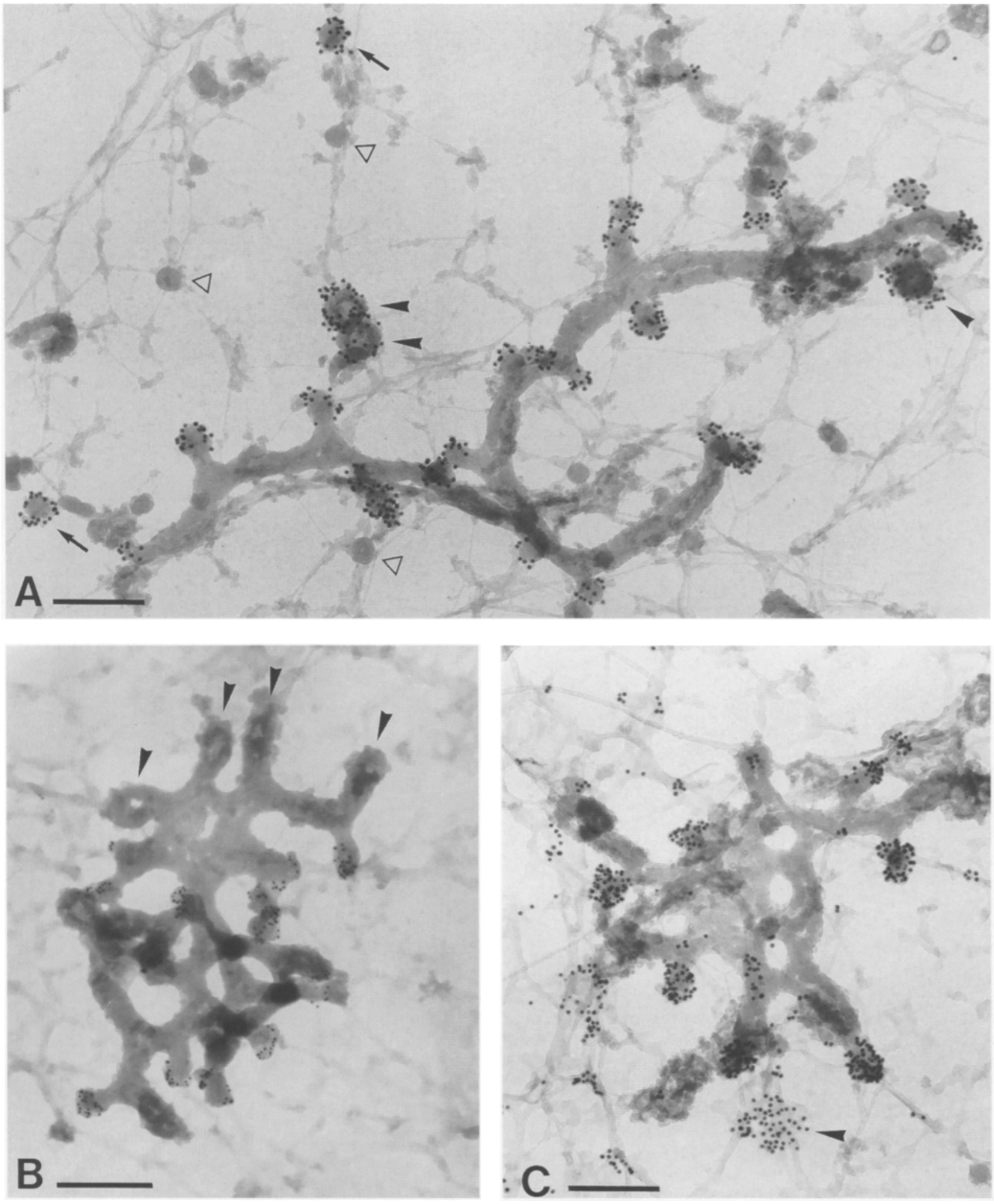

Figure 4. Endosome derived clathrin-coated vesicles. Cells were labeled with Tf/HRP and processed as in Fig. 3 *A*. After permeabilization and fixation, the cells were immuno–double-labeled with protein A complexed to 5-nm and 10-nm gold particles. (*A*). Cells were labeled with 10-nm gold for the demonstration of clathrin heavy chain using the monoclonal X22. A peripheral tubular DAB-labeled endosome continuous with many 60-nm clathrin-coated buds is shown. Free DAB-positive vesicles with a diameter of 60 nm and labeled for clathrin (*arrows*) probably derived from the endosome. Non–clathrin-coated DAB-labeled 60-nm vesicles (possibly representing uncoated endosome-derived vesicles; *triangles*) and DAB-positive 100-nm clathrin-coated vesicles, discontinuous with the endosome and presumably derived from the plasma membrane (*arrowheads*) are also present. (*B*) Cells were labeled with 5-nm gold for the demon-

technique, we checked for the integrity of endosomal tubules after BFA treatment. A431 cells were incubated for 60 min at 37°C in the presence of Tf/HRP to ensure labeling of the entire endocytic tract of TfR with peroxidase activity. BFA was either omitted or present during the last 1–30 min of this incubation. Subsequently, the cells were prepared for whole-mount electron microscopy. Individual electron-lucent cells were observed with a contrasted nucleus, and electron-dense DAB polymer deposited at the perinuclear area and cell periphery (Fig. 3 *A*). In the absence of BFA, hundreds of individual DAB-labeled endosomes were encountered in the periphery of each cell (Fig. 3 *B*). We did not find DAB-labeled organelles after DAB cytochemistry on unfixed A431 cells when Tf/HRP was omitted (not shown). Besides their DAB contents, endosomes were also identified by the presence of TfR as shown by abundant immuno–gold labeling (see Fig. 6). Endosomes were of variable shapes and sizes and consisted of interconnected tubules only or tubules connected to vacuoles. The lengths of these tubular endosomes varied from 100 nm to 3 μm. Besides peripheral endosomes, many DAB-positive structures were found in the perinuclear area packed so densely that the continuity between these structures could not easily be determined (see Fig. 1 *A*; for higher magnification, see Fig. 5 *D*). After 1 min in the presence of BFA, a significant increase in the average length of endosomal tubules was already detected (not shown). After 5 min a large continuous DAB-stained endosomal network was found (Fig. 3 *C*), consistent with observations by others (Lippincott-Schwartz et al., 1991; Wood et al., 1991; Hunziger et al., 1991). After a prolonged incubation in the presence of BFA (up to 30 min), tubular endosomes disappeared from the periphery of the cell and redistributed to the perinuclear area (not shown). Similar observations were made for the human hepatoma cell line HepG2, and the human epidermoid carcinoma cell line Hep2 (not shown). These data show that endosomal tubules, when present, were not fragmented during sample preparation. Thus, it must be concluded that at normal cell culture conditions endosomes do not form a continuous membranous network.

Endosomal Buds Coated with Clathrin

On each individual endosome, buds with a uniform diameter of 60 nm were observed. Labeling of whole-mount cells with antibodies to clathrin light chain from three different sources and to clathrin heavy chain from two different sources (see *Materials and Methods*) revealed that both heavy and light chain clathrin are associated with these buds (Fig. 4, *A* and *C*). The continuity of these buds with endosomes was confirmed by stereo images (not shown). Besides 60-nm clathrin-labeled buds, occasionally 80–100-nm buds that did not label for clathrin were also found associated with endosomes (Fig. 4 *B*, *arrowheads*). In addition to clathrin-coated buds on endosomes, free 60-nm DAB-labeled clathrin-coated vesicles were encountered (Fig. 4 *A*, *open triangles*). The endosome-associated clathrin-coated buds and free DAB-labeled clathrin-coated vesicles were considerably smaller than plasma membrane–derived 100-nm clathrin-coated vesicles (Figs. 4 *A*, *arrowheads* indicate 100-nm clathrin-coated vesicles; for labeling with anti–α-adaptin see Figs. 2 and 5 *A*). After a 5-min incubation in the presence of BFA, clathrin-coated buds were absent on the tubular endosomal network (not shown), indicating that their formation was inhibited by this drug.

To further discriminate endosome-associated clathrin-coated buds from plasma membrane–derived clathrin-coated vesicles, we immuno–double-labeled for α-adaptin and clathrin (5 nm and 10 nm gold, respectively; Figs. 5, *A* and *B*). Generally, endosome-associated clathrin-coated buds were negative for α-adaptin (Fig. 5 *A*). Occasionally, however, little labeling for α-adaptin was found on clathrin-labeled buds on endosomes (Fig. 5 *B*, *arrowheads*), confirming that some α-adaptin may be associated with endosomes (Wang et al., 1993; Seaman et al., 1993). In contrast, plasma membrane–derived DAB-labeled 100-nm clathrin-coated vesicles (Fig. 5 *A*, *arrow*) labeled heavily for α-adaptin. α-adaptin was also found on clathrin-labeled, DAB-negative sites, representing clathrin-coated pits at the plasma membrane (Fig. 5 *A*, *arrowhead*). Endosome-associated clathrin-coated buds were thus discriminated from plasma membrane–derived coated vesicles by their continuity with endosomes, the absence of α-adaptin, and their size.

To discriminate endosome-associated clathrin-coated buds from TGN-derived coated vesicles, we immuno–double-labeled for clathrin and γ-adaptin. Recycling endosomes and the TGN are localized in the perinuclear area and are closely associated with one another (Hopkins et al., 1994; Connolly et al., 1994). A dense mass of 60-nm DAB-labeled tubules was found in the perinuclear area (Fig. 5 *D*), analogous to the recycling endosomes reported by others (Ghosh and Maxfield, 1995; Hopkins et al., 1994; Connolly et al., 1994). DAB-negative vesicles, labeled for clathrin (10 nm gold) and γ-adaptin (5 nm gold), were also found in this area (Fig. 5 *D*, *arrows*) and are characteristic for TGN-derived clathrin-coated vesicles (Geuze and Morré, 1991; Klumperman et al., 1993). Due to the lack of contrast of DAB-negative membranes, the diameter of these vesicles could not be measured. However, in cryosections they have a diameter of ~100 nm (Klumperman et al., 1993), similar to that of plasma membrane–derived clathrin-coated vesicles. In contrast to perinuclear clathrin-coated buds/vesicles, endosome-associated clathrin-coated buds were largely negative for γ-adaptin (Fig. 5 *C*). Occasionally, some γ-adaptin was detected on endosome-associated clathrin-coated buds (Fig. 5 *C*, *arrowheads*). We conclude that endosome-associated clathrin-coated pits can be discerned from TGN-derived coated vesicles by their subcellular localization, size, and the absence of γ-adaptin.

stration of clathrin light chain using the monoclonal CON.1. A peripheral tubular DAB-labeled endosome continuous with many 60-nm clathrin-coated buds is shown. In addition, 100-nm buds that are not labeled for clathrin can be seen (*arrowheads*). (*C*) Cells were immuno–double-labeled to demonstrate the simultaneous presence of clathrin light chain (polyclonal Ungewickell; 5-nm gold) and clathrin heavy chain (monoclonal X22; 10-nm gold) on DAB-labeled endosome-associated buds. Note the 100-nm DAB-negative clathrin-coated pit or clathrin lattice at the plasma membrane (*arrowhead*). Bars, 0.2 μm.

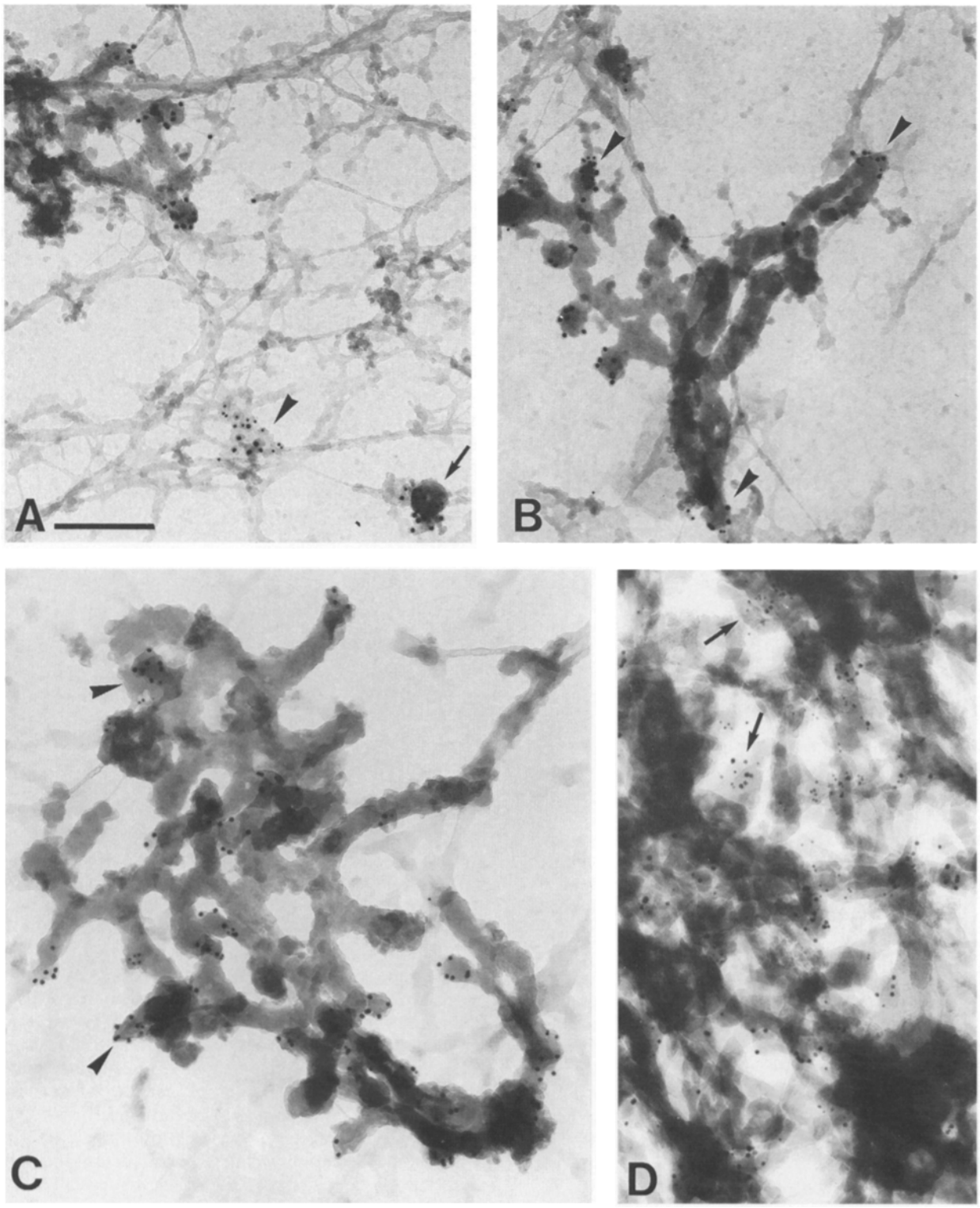

Figure 5. Endosome-derived clathrin-coated vesicles can be differentiated from plasma membrane– and TGN-derived clathrin-coated vesicles by the absence of α- and γ-adaptin. Cells were labeled with Tf/HRP and processed as in Fig. 3 *A*. After permeabilization and fixation, the cells were immuno–double-labeled with protein A complexed to 5-nm and 10-nm gold particles. (*A* and *B*) Cells were double-labeled with 5-nm and 10-nm gold for the demonstration of α-adaptin and clathrin light chain (polyclonal Ungewickell), respectively. (*A*) Peripheral tubular DAB-positive endosome continuous with 60-nm clathrin-coated buds that are negative for α-adaptin is shown. In contrast, a DAB-negative clathrin-coated pit at the plasma membrane (*arrowhead*) and a 100-nm DAB-positive plasma membrane–derived clathrin-coated vesicle (*arrow*) are labeled for α-adaptin. (*B*) Occasionally, 60-nm clathrin-coated buds on peripheral endosomes labeled for α-adaptin (*arrowheads*). (*C* and *D*) Cells were double-labeled with 5-nm and 10-nm gold for the demonstration of γ-adaptin and clathrin light chain (polyclonal Ungewickell), respectively. (*C*) Only occasionally 60-nm clathrin-coated buds on peripheral endosomes labeled for γ-adaptin (*arrowheads*). (*D*) In the perinuclear area many densely packed DAB-positive membranes were observed. Between this dense material, DAB-negative vesicles with an apparent diameter of 60 nm labeled for clathrin and γ-adaptin (*arrows*).

Endosome-associated 60-nm Buds Contain TfR

Analogous to plasma membrane– and TGN-derived clathrin-coated vesicles, endosome-derived clathrin-coated vesicles may be expected to carry a selected cargo of integral membrane proteins. We studied whether endosome-associated buds are labeled for TfR as a representative for the recycling pathway. Antibodies directed against the cytoplasmic tail of the TfR were used to avoid epitopes that may have been masked by the DAB polymer. Only little TfR labeling (10 nm gold) in clathrin-coated buds (5 nm gold) as compared to the rest of the endosome was found (Fig. 6 *B*, *arrowheads*). We anticipated that, due to steric hindrance, the clathrin coat interfered with labeling of the cytoplasmic tail of the TfR. To avoid this problem, we removed clathrin coats by incubating the saponin-permeabilized cells in 0.5 M Tris before the paraformaldehyde fixation. This procedure, originally developed to strip clathrin coats from isolated plasma membranes (Mahaffey et al., 1990), efficiently removed clathrin from endosomes and the plasma membrane (not shown). The typical 60-nm buds on endosomes (Fig. 6 *A*, *arrowheads*), stripped from clathrin, now efficiently labeled for TfR (Fig. 6 *A*, 5 nm gold). To determine whether TfR was specifically incorporated in these buds, the distribution of MPR, an integral membrane protein sorted from the TfR in endosomes to be transported to the TGN, was also assessed. We were not able to detect a selective enrichment of TfR (5 nm gold) nor MPR (10 nm gold) in endosome-associated 60-nm buds (Fig. 6 *A*). However, an enrichment of TfR in clathrin-coated buds by only 5% may already be sufficient for efficient recycling (see *Discussion*). In the presence of BFA, an endosomal network devoid of clathrin-coated buds was formed (Fig. 6 *C*). This network was homogeneously labeled for TfR (5 nm gold) and MPR (10 nm gold). No lateral heterogeneity in the distribution of these proteins along these tubules was observed. Concurrent with the disappearance of clathrin-coated buds on endosomes in the presence of BFA, the expression of the TfR at the plasma membrane decreased twofold due to a relatively low externalization rate (unpublished data; see also Damke et al., 1991; Schonhorn et al., 1994). This suggested that endosome-derived clathrin-coated vesicles are involved in TfR recycling.

Discussion

We identified an exit from endosomes involving a novel class of clathrin-coated vesicles. These clathrin-coated vesicles were distinguished from those originating from the plasma membrane and the TGN. Clathrin-coated buds on endosomes were visualized using a novel technique that allows for whole-mount immunoelectron microscopy of the endosomal apparatus at the electron microscopic level. It involves the selective fixation of endosomes with DAB polymer by using the peroxidase activity of endocytosed Tf/HRP. DAB polymerization by extracellular Tf/HRP was suppressed selectively using ascorbic acid (Figs. 1 and 6), yielding DAB staining of Tf/HRP-labeled endosomes only (Fig. 3). Endosomes are comprised of vacuolar and tubular elements that localize to the periphery and in the perinuclear area of the cells consistent with earlier observations (Geuze et al., 1983; Hopkins et al., 1990). Both peripheral and perinuclear tubular DAB-labeled endosomes had a diameter of 60 nm, analogous to diameters reported by others (Hopkins and Trowbridge 1983; Tooze and Hollinshead, 1991; Hopkins et al., 1994).

After the initial realization that endocytosed proteins are sorted in a prelysosomal compartment which is composed of vesicular elements with attached tubular extensions (Geuze et al., 1983), endosomal tubules with lengths ≥ 2 μm have been observed in electron microscopic images of thick sections of HRP-labeled cells (Tooze and Hollinshead, 1991), and in three-dimensional reconstructions using serial thin sections (Marsh et al., 1986). Although already considerable, the tubule length in these studies may have been limited artificially due to fragmentation after chemical fixation (Hopkins et al., 1990; Robinson and Karnovsky, 1991). Light microscopic images of living cells incubated with fluorescently labeled transferrin suggested that nonfixed endosomes may even form a continuous network (Hopkins et al., 1990). However, our electron microscopic images of nonsectioned DAB-fixed endosomes confirmed the earlier observations that endosomes do not form a continuous membranous network (see Fig. 2). In the present study, the tubular aspect of endosomes had been preserved well during preparation since BFA-induced tubular endosomal networks were not disrupted (Fig. 2 *B*). In addition, in the absence of BFA, the tips of endosomal tubules were often coated with clathrin, which cannot be explained when tubules would have been fragmented during the treatment. Although not continuously connected with one another, endosomes might form transient networks by fusion and fission events (Gruenberg and Howell, 1989). Such transient connections may contribute to the visualization of an apparent continuous network in living cells at the light microscopic level (Hopkins et al., 1990).

Cytoplasmic tails of integral membrane proteins in endosomes, and proteins associated with the cytoplasmic face of endosomes were immunolabeled using colloidal gold. Numerous clathrin-coated buds continuous with endosomal vacuoles and tubules were detected. In previous studies, clathrin has occasionally been found associated with endosomes (Geuze et al., 1983; Killish et al., 1992). Unidentified coats on presumed endosomes have also been reported previously (Geuze et al., 1984; Allen et al., 1992; Rabinowitz et al., 1992). However, in these studies endosome-associated clathrin coats were scarce and were not discerned from plasma membrane– and TGN-derived clathrin-coated membranes. In our opinion, the best marker available, generally thought to be highly enriched on TGN and not on endosomes, is γ-adaptin (Robinson, 1994). Similarly, AP2 is a specific marker for plasma membrane–derived clathrin-coated vesicles. On cryosections of cells, limited immunolabeling for AP1 and AP2 does not allow for the identification of endosome-associated clathrin-coated buds negative for AP1 or AP2. In contrast, the novel technique described here allows for immunolabeling of the entire surface of endosomes, thereby achieving a high labeling efficiency. This allowed us to discriminate clearly between γ-adaptin-labeled and γ-adaptin-negative clathrin-coated buds (Fig. 5, *C* and *D*). Thus, endosome-associated clathrin-coated buds could be discerned from TGN-derived coated vesicles by the absence of γ-adaptin and localization in the

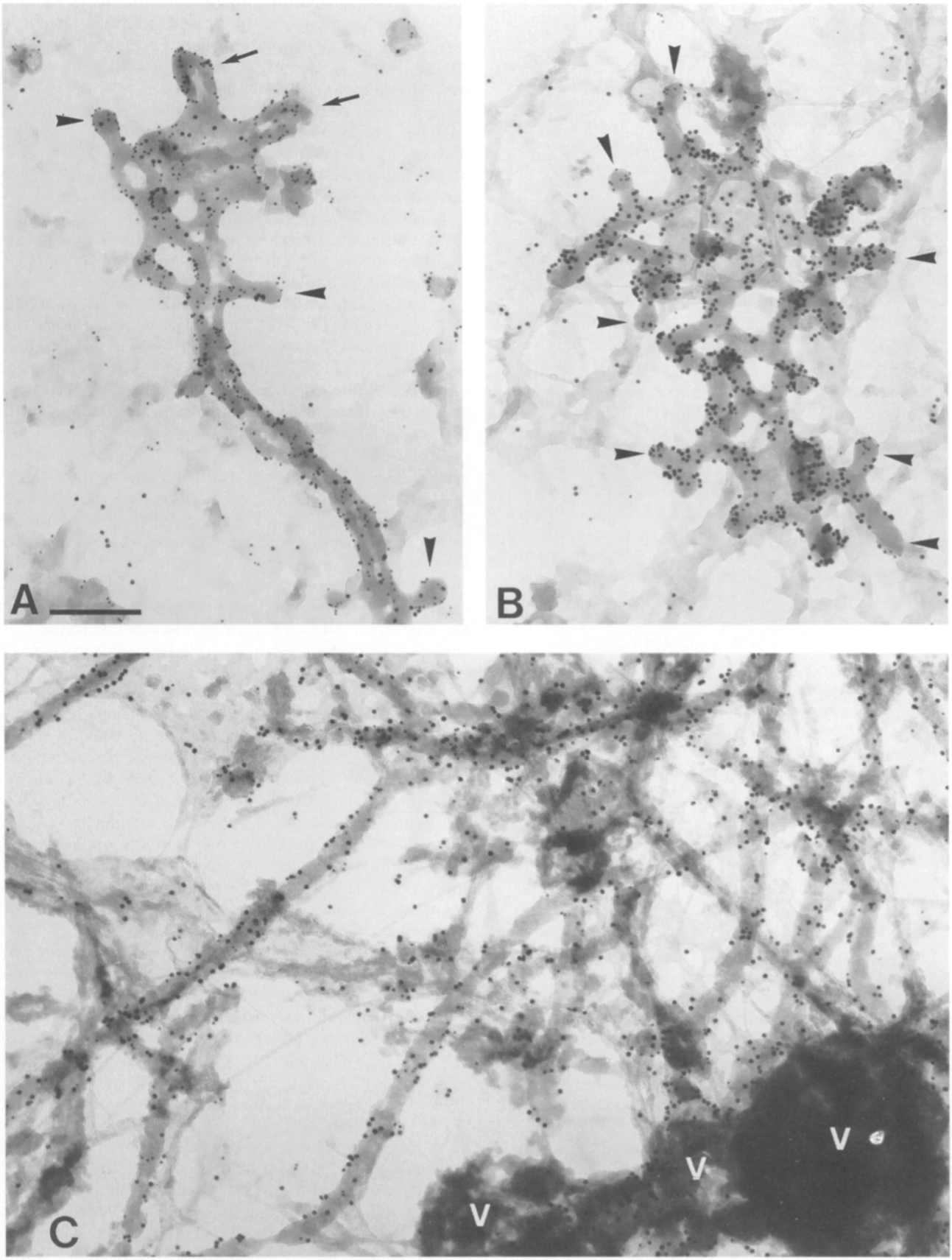

Figure 6. Incorporation of TfR in endosomal buds. Cells were labeled with Tf/HRP and processed as in Fig. 3 *A*. (*A*) After permeabilization, the cells were washed with 0.5 M Tris to remove clathrin coats before fixation. The cells were immuno–double-labeled for TfR and MPR using 5-nm and 10-nm gold particles, respectively. Both 60-nm (*arrowheads*) and 100-nm buds (*arrows*) were labeled for TfR

cell. In addition, TGN-derived coated vesicles have a diameter of ~100 nm (Klumperman et al., 1993), which is significantly larger than the 60-nm endosome-associated clathrin-coated buds. The clathrin-coated buds on endosomes were also discerned from plasma membrane–derived coated vesicles by three criteria: size (60 nm and 100 nm, respectively), the absence of α-adaptin, and continuity with endosomes (Figs. 2 and 5 *A*). Only occasionally γ-adaptin (Fig. 5 *C*) and α-adaptin (Fig. 5 *B*) were found associated with peripheral Tf/HRP-labeled endosomes. In contrast, clathrin-coated vesicles derived from the plasma membrane and TGN labeled heavily for α-adaptin (Fig. 5 *A*) and γ-adaptin (Fig. 5 *D*), respectively. Apparently, γ-adaptin and α-adaptin are not exclusively localized at the TGN and the plasma membrane. The potential of AP2 to be targeted to endosomes was also illustrated by the localization of AP2 on endosomes in the presence of cationic amphiphilic drugs (Wang et al., 1993) and in the presence of GTPγS or excess Ca^{2+} (Seaman et al., 1993). Overexpression of TGN 38/41, a TGN protein binding to AP1 adaptors, led to mislocalization of γ-adaptin to endosomes (Reaves and Banting, 1994). Adaptors are thought to be recruited from the cytosol to specific membranes by largely unidentified adaptor receptors (Moore et al., 1987; Mahaffey et al., 1990; Stamnes and Rothman, 1993; Traub et al., 1993). Possibly, residual interactions between adaptors and their receptors in endosomes may explain the minor amounts of α-adaptin and γ-adaptin found on endosomes in the current study. Alternatively, adaptors may play a role in the docking of vesicles with endosomes (Beck et al., 1992). Finally, the antibodies directed against γ-adaptin and/or α-adaptin may cross-react with unidentified endosome-associated adaptins.

Endosome-derived clathrin coated vesicles may be associated with yet unidentified adaptor complexes. In the nerve endings of neuronal cells, a clathrin assembly protein, AP180, has been characterized to induce the assembly of clathrin in 60–70-nm coats (Morris et al., 1993, and references therein). Two other potential novel adaptor proteins, p47A and p47B, which show homology with the 50- and 47-kD subunits of the AP1 and AP2 adaptor complexes have been characterized (Pevsner et al., 1994). Although the physiological functions of these proteins are unknown they may serve as adaptor subunits in the generation of clathrin-coated vesicles at endosomes.

Why have endosome-associated clathrin-coated buds not been frequently encountered by immunocytochemistry on cryosections? One plausible explanation could be that clathrin-coated buds on endosomes may be relatively unstable and dissociate before chemical fixation with formaldehyde or glutaraldehyde. This notion is supported by the occasional detection of relatively high cytosolic clathrin concentrations close to, but not in contact with, endosomal tubules on cryosections (Geuze et al., 1983). HRP-driven cross-linking of endosomal integral membrane proteins to DAB polymer may preserve the cytoplasmic tails for adaptor/clathrin binding. Indeed, we found that nonfixed clathrin cages were stably associated with DAB-fixed endosomes during the saponin incubation, even in PBS lacking Mg^{2+} and EGTA (not shown).

The pathway(s) served by endosome-derived clathrin-coated vesicles remain speculative at this time. Previously, we showed that although TfR and MPR are enriched in early and late endosomes, respectively, the endosomal distributions revealed an extensive overlap (Stoorvogel et al., 1991*b*). In the present study, we found labeling of both MPR and TfR in early endosome-associated clathrin-coated buds, but were not able to determine whether one of these antigens is selectively enriched in these structures. Epitopes on the cytoplasmic tails of these proteins were masked by the clathrin/adaptor coat for antibody binding (Fig. 6 *B*). However, stripping of the clathrin coat from these buds in 0.5 M Tris allowed access to the epitopes (Fig. 6 *A*). Stripped endosomal 60-nm buds were heavily labeled for TfR, but MPR was not excluded. In these preparations, epitope accessibility may still suffer from steric hindrance due to dense packing of integral membrane proteins. Thus, no definite conclusions regarding the selectivity for incorporation of integral membrane proteins in endosomal 60-nm buds could be made. However, several findings argue in favor of the possibility that endosome-derived clathrin-coated vesicles are involved in the recycling pathway. First, clathrin-coated buds on endosomes are heavily labeled with DAB polymer and thus contain significant amounts of TfR-Tf/HRP. Second, after the Tris wash all 60-nm buds on endosomes labeled heavily for the TfR. Third, clathrin-coated buds are quite numerous on typical peripheral early endosomes, organelles considered to sort recycling proteins from lysosomal targeted proteins. Fourth, BFA concomitantly inhibited TfR recycling and the formation of clathrin-coated buds at endosomes. BFA interferes with the association of the cytoplasmic tail of MPR with AP1 (LeBorgne et al., 1993), resulting in a two- to fourfold increase of its expression at the plasma membrane due to an increased externalization rate (Damke et al., 1991). In contrast, the expression of the TfR at the plasma membrane decreases twofold due to a relatively low externalization rate (unpublished data; see also Damke et al., 1991; Schonhorn and Wessling-Resnick, 1994). Endocytosed TfR exits the sorting endosome within 1–2 min after uptake whereas the entire endocytic cycle takes ~10 min (Stoorvogel et al., 1987). Thus, the exit from endosomes does not constitute the rate-limiting step of the TfR cycle through the cell. Consequently, inhibition of the egress of TfR from endosomes by BFA would need to be very effective (~10 times) to achieve the measured twofold increase in the rate of recycling of the TfR. Concurrent with the inhibitory effect of BFA on TfR recycling, clathrin-coated buds disap-

and MPR. Label not associated with DAB polymer probably localizes to the plasma membrane. (*B*) Cells that were not washed with Tris before fixation were immuno–double-labeled for clathrin light chain (CON.1) and TfR using 5-nm and 10-nm gold particles, respectively. TfR was not labeled efficiently on 60-nm clathrin-coated buds on endosomes (*arrowheads*). (*C*) During the last 5 min of Tf/HRP uptake, BFA was present in the medium. The cells were immuno–double-labeled for TfR and MPR using 5-nm and 10-nm gold particles, respectively. Extensive labeling for both proteins was found along the entire length of the endosomal tubules. Note the large DAB-positive vacuoles (*V*) that also labeled for both proteins. Bar in *A*, 0.2 μm, is representative for all figures.

peared from endosomes (Fig. 6 *C*), suggesting their involvement in TfR recycling. In Dictiostelium there is genetic evidence for the involvement of clathrin in the secretion of mature α-mannosidase from lysosomes to the extracellular space (Ruscetti et al., 1994). This secretion is thought to occur via a postlysosomal compartment (Padh et al., 1993), possibly equivalent to endosomes.

An alternative function for endosome-derived clathrin-coated vesicles, which cannot be excluded, is that they serve transport from endosomes to the TGN. Although endocytosed MPR is targeted first to early endosomes, its sorting from the endocytic pathway is considered to occur mainly at late endosomes (Stoorvogel et al., 1989; Riederer et al., 1994). Thus, it appears unlikely that clathrin-coated buds that are formed in great numbers at early endosomes serve a pathway from endosomes to the TGN. In addition, the finding by Draper et al. (1990) that, in permeabilized cells, anti-clathrin antibodies did not interfere with the trafficking of MPR from endosomes to the TGN also argues against this possibility.

Besides 60-nm clathrin-coated buds, 100-nm buds lacking clathrin were also found on endosomes (Fig. 3 *A*). These buds labeled for both TfR and MPR (Fig. 6 *A*). Unlike the 60-nm buds, 100-nm buds did not require a treatment with 0.5 M Tris to be labeled for these proteins (not shown), suggesting that these buds are either not coated or contain a nonclathrin coat that did not interfere with antigen accessibility. Since these buds have the same diameter as plasma membrane–derived coated vesicles and TGN-derived clathrin-coated vesicles (Klumperman et al., 1993), they may represent the fusion site for uncoated plasma membrane–derived or TGN-derived vesicles. Alternatively, they may represent the budding site for nonidentified transport vesicles. Recently, ARF6 has been implicated in vesicular transport between the plasma membrane and endosomes (Peters et al., 1995; D'Souza-Schorey et al., 1995). Overexpression of a dominant negative ARF6 mutant, defective in GTP binding, resulted in impaired recycling of endocytosed transferrin (D'Souza-Schorey et al., 1995) and the accumulation of 100–300-nm vesicles with an unidentified coat lacking clathrin (Peters et al., 1995). These vesicles could represent either unfused endocytic structures that have either acquired or revealed a new coat, or recycling endosomal remnants (Peters et al., 1995), and may be equivalent to the 100-nm buds identified in the present study.

In conclusion, we identified a novel class of clathrin-coated vesicles budding from endosomes, via which recycling to the plasma membrane may occur. Further evidence is required to positively identify endosome-derived clathrin-coated vesicles as transport intermediates in this pathway.

We thank René Scriwanek for dark room services, and Brigitte Groothuis for technical assistance. We are grateful to Dr. Trowbridge, Dr. Ungewickell, Dr. Keen, Dr. Brodsky, and Dr. Robinson for their gifts of antibodies.

These investigations were sponsored by a senior investigatorship from the Royal Netherlands Academy of Arts and Sciences.

Received for publication 24 July 1995 and in revised form 2 October 1995.

References

Ahle, S., A. Mann, U. Eichelsbacher, and E. Ungewickell. 1988. Structural relationships between clathrin assembly proteins from the Golgi and the plasma membrane. *EMBO (Eur. Mol. Biol. Organ.) J.* 7:919–929.

Allen, R. D., C. C. Schroeder, and A. K. Fok. 1992. Endosomal system in paramecium: coated pits to early endosomes. *J. Cell Sci.* 101:449–461.

Barlowe, C., L. Orci, T. Yeung, M. Hosobuchi, S. Hamamoto, N. Salama, M. F. Rexach, M. Ravazzola, M. Amherdt, and R. Schekman. 1994. COP II: a membrane coat formed by Sec proteins that drive vesicle budding from the endoplasmic reticulum. *Cell.* 77:895–907.

Beck, K. A., M. Chang, F. M. Brodsky, and J. H. Keen. 1992. Clathrin assembly protein AP-2 induces aggregation of membrane vesicles: a possible role for AP-2 in endosome formation. *J. Cell Biol.* 119:787–796.

Brodsky, F. M. 1985. Clathrin structure characterized with monoclonal antibodies. I. Analysis of multiple antigenic sites. *J. Cell Biol.* 101:2047–2054.

Chin, D. J., R. M. Straubinger, S. Acton, I. Näthke, and F. M. Brodsky. 1989. 100-kDa polypeptides in peripheral clathrin-coated vesicles are required for receptor-mediated endocytosis. *Proc. Natl. Acad. Sci. USA.* 86:9289–9293.

Connolly, C. N., C. E. Futter, A. Gibson, C. R. Hopkins, and D. F. Cutler. 1994. Transport into and out of the Golgi complex studied by transfecting cells with cDNAs encoding horseradish peroxidase. *J. Cell Biol.* 127:641–652.

Courtoy, P. J. 1991. Dissection of endosomes. *In* Intracellular Trafficking of Proteins. J. C. Steer and J. Harford, editors. Cambridge University Press, New York. 103–156.

Courtoy, P. J., J. Quintart, and P. Baudhuin. 1984. Shift of equilibrium density induced by 3,3′-diaminobenzidine cytochemistry: a new procedure for the analysis and purification of peroxidase-containing organelles. *J. Cell Biol.* 98: 870–876.

Damke, H., J. Klumperman, K. von Figura, and T. Braulke. 1991. Effects of brefeldin A on the endocytic route. Redistribution of mannose 6-phosphate/insulin-like growth factor II receptors to the cell surface. *J. Biol. Chem.* 266: 24829–24833.

Doms, R. W., G. Russ, and J. W. Yewdell. 1989. Brefeldin A redistributes resident and itinerant Golgi proteins to the endocytic reticulum. *J. Cell Biol.* 109:61–72.

Dourmashkin, R. R., R. M. Dougherty, and R. J. C. Harris. 1962. Electron microscopic observations on Rous sarcoma virus and cell membranes. *Nature (Lond.).* 194:1116–1119.

Draper, R. K., Y. Goda, F. M. Brodsky, and S. R. Pfeffer. 1990. Antibodies to clathrin inhibit endocytosis but not recycling to the trans-Golgi network in vitro. *Science (Wash. DC).* 248:1539–1541.

D'Souza-Schorey, C., G. Li, M. I. Colombo, and P. D. Stahl. 1995. A regulatory role for ARF6 in receptor-mediated endocytosis. *Science (Wash. DC).* 267: 1175–1178.

Felder, S., K. Miller, G. Moehren, A. Ullrich, J. Schlessinger, and C. R. Hopkins. 1990. Kinase activity controls the sorting of the epidermal growth factor receptor within the multivesicular body. *Cell.* 61:623–634.

Fujiwara, T., K. Oda, S. Yokoda, A. Takatsuki, and Y. Ikehara. 1988. Brefeldin A causes disassembly of the Golgi complex and accumulation of secretory proteins in the endoplasmic reticulum. *J. Biol. Chem.* 263:18545–18552.

Fukuda, M. 1991. Lysosomal membrane glycoproteins. Structure, biosynthesis, and intracellular trafficking. *J. Biol. Chem.* 266:21327–21330.

Futter, C. E., S. Felder, J. Schlessinger, A. Ullrich, and C. R. Hopkins. 1993. Annexin I is phosphorylated in the multivesicular body during the processing of the epidermal growth factor receptor. *J. Cell Biol.* 120:77–83.

Geuze, H. J., J. W. Slot, G. J. Strous, H. F. Lodish, and A. L. Schwartz. 1983. Intracellular site of asialoglycoprotein receptor-ligand uncoupling: double-label immunoelectron microscopy during receptor-mediated endocytosis. *Cell.* 32:277–287.

Geuze, H. J., J. W. Slot, G. J. Strous, J. Peppard, K. von Figura, A. Hasilik, and A. L. Schwartz. 1984. Intracellular receptor sorting during endocytosis: comparative immunoelectron microscopy of multiple receptors in rat liver. *Cell.* 37:195–204.

Geuze, H. J., J. W. Slot, and A. L. Schwartz. 1987. Membranes of sorting organelles display lateral heterogeneity in receptor distribution. *J. Cell Biol.* 104:1715–1723.

Geuze, H. J., and D. J. Morré. 1991. Trans-Golgi reticulum. *J. Electron Microsc.* 17:24–34.

Ghosh, R. N., and F. R. Maxfield. 1995. Evidence for nonvectorial, retrograde transferrin trafficking in the early endosomes of HEp2 cells. *J. Cell Biol.* 128: 549–561.

Gruenberg, J., and K. E. Howell. 1989. Membrane traffic in endocytosis: insights from cell-free assays. *Annu. Rev. Cell Biol.* 5:453–481.

Guarnieri, F. G., L. M. Arterburn, M. B. Penno, Y. Cha, and J. T. August. 1993. The motif tyr-x-x-hydrophobic residue mediates lysosomal membrane targeting of lysosome-associated membrane protein 1. *J. Biol. Chem.* 268:1941–1946.

Hopkins, C. R., and I. S. Trowbridge. 1983. Internalization and processing of transferrin and the transferrin receptor in human carcinoma A431 cells. *J. Cell Biol.* 97:508–521.

Hopkins, C. R., A. Gibson, M. Shipman, and K. Miller. 1990. Movement of internalized ligand-receptor complexes along a continuous endosomal reticulum. *Nature (Lond.).* 346:335–339.

Hopkins, C. R., A. Gibson, M. Shipman, D. K. Strickland, and I. S. Trowbridge. 1994. In migrating fibroblasts, recycling receptors are concentrated in narrow tubules in the pericentriolar area, and then routed to the plasma membrane of the leading lamella. *J. Cell Biol.* 125:1265–1274.

Hunziger, W., J. A. Whitney, and I. Mellman. 1991. Selective inhibition of trans-

cytosis by brefeldin A in MDCK cells. *Cell.* 64:617–627.
Keen, J. H. 1990. Clathrin and associated assembly and disassembly proteins. *Annu. Rev. Biochem.* 59:415–438.
Killisch, I., P. Steinlein, K. Römisch, R. Hollinshead, H. Beug, and G. Griffiths. 1992. Characterization of early and late endocytic compartments of the transferrin cycle. Transferrin receptor antibody blocks erythroid differentiation by trapping the receptor in the early endosome. *J. Cell Sci.* 103:211–232.
Klumperman, J., A. Hille, T. Veenendaal, V. Oorschot, W. Stoorvogel, K. von Figura, and H. J. Geuze. 1993. Differences in the endosomal distributions of the two mannose 6-phosphate receptors. *J. Cell Biol.* 121:997–1010.
LeBorgne, R., A. Schmidt, F. Mauxion, G. Griffiths, and B. Hoflack. 1993. Binding of AP-1 Golgi adaptors to membranes requires phosphorylated cytoplasmic domains of the mannose 6-phosphate/insulin-like growth factor II receptor. *J. Biol. Chem.* 268:22552–22556.
Lippincott-Schwartz, J., L. C. Yuan, J. S. Bonifacino, and R. D. Klausner. 1989. Rapid redistribution of Golgi proteins into the ER in cells treated with brefeldin A: evidence for membrane cycling from Golgi to ER. *Cell.* 56:801–813.
Lippincott-Schwartz, J., L. Yuan, C. Tipper, M. Amherdt, L. Orci, and R. D. Klausner. 1991. Brefeldin A's effects on endosomes, lysosomes, and the TGN suggest a general mechanism for regulating organelle structure and membrane traffic. *Cell.* 67:601–616.
Luzio, J. P., and G. Banting. 1993. Eukaryotic membrane traffic: retrieval and retention mechanisms to achieve organelle residence. *Trends Biochem. Sci.* 18:395–398.
Mahaffey, D. T., J. S. Peeler, F. M. Brodsky, and R. G. W. Anderson. 1990. Clathrin-coated pits contain an integral membrane protein that binds the AP-2 subunit with high affinity. *J. Biol. Chem.* 265:16514–16520.
Marsh, M., G. Griffiths, G. E. Dean, I. Mellman, and A. Helenius. 1986. Three-dimensional structure of endosomes in BHK-21 cells. *Proc. Natl. Acad. Sci. USA.* 83:2899–2903.
Moore, M. S., D. T. Mahaffey, F. M. Brodsky, and R. G. W. Anderson. 1987. Assembly of clathrin-coated pits onto purified plasma membranes. *Science (Wash. DC).* 236:558–563.
Morris, S. A., S. Schröder, U. Plessman, K. Weber, and E. Ungewickell. 1993. Clathrin assembly protein AP180: primary structure, domain organization and identification of a clathrin binding site. *EMBO (Eur. Mol. Biol. Organ.) J.* 12:667–675.
Näthke, I. S., J. Heuser, A. Lupas, J. Stock, C. W. Turck, and F. M. Brodsky. 1992. Folding and trimerization of clathrin subunits at the triskelion hub. *Cell.* 68:899–910.
Padh, H., J. Ha, M. Lavasa, and T. L. Steck. 1993. A post-lysosomal compartment in Dictyostelium discoideum. *J. Biol. Chem.* 268:6742–6747.
Pearse, B., and M. Robinson. 1990. Clathrin, adaptors and sorting. *Annu. Rev. Cell Biol.* 6:151–171.
Peters, P. J. V. W. Hsu, C. Eng Ooi, D. Finazzi, S. B. Teal, V. Oorschot, J. G. Donaldson, and R. D. Klausner. 1995. Overexpression of wild-type and mutant ARF1 and ARF6: distinct perturbations of nonoverlapping membrane compartments. *J. Cell Biol.* 128:1003–1017.
Pevsner, J., W. Volknandt, B. R. Wong, and R. H. Scheller. 1994. Two rat homologs of clathrin-associated adaptor proteins. *Gene.* 146:279–283.
Rabinowitz, S., H. Horstmann, S. Gordon, and G. Griffiths. 1992. Immunocytochemical characterization of the endocytic and phagolysosomal compartments in peritoneal macrophages. *J. Cell Biol.* 116:95–112.
Randazzo, P. A., Y. C. Yang, C. Rulka, and R. A. Kahn. 1993. Activation of ADP-ribosylation factor by Golgi membranes: evidence for a brefeldin A- and protease-sensitive activating factor on Golgi membranes. *J. Biol. Chem.* 268:9555–9563.
Reaves, B., and G. Banting. 1994. Overexpression of TGN38/41 leads to mislocalization of γ-adaptin. *FEBS (Fed. Eur. Biochem. Soc.) Lett.* 351:448–456.
Riederer, M. A., T. Soldati, A. D. Shapiro, J. Lin, and S. R. Pfeffer. 1994. Lysosome biogenesis requires rab9 function and receptor recycling from endosomes to the *trans*-Golgi network. *J. Cell Biol.* 125:573–582.
Rijnboutt, S., H. M. F. G. Aerts, H. J. Geuze, J. M. Tager, and G. J. Strous. 1991. Mannose 6-phosphate-independent membrane-association of cathepsin D, glucocerebrosidase and sphingolipid activating protein in HepG2 cells. *J. Biol. Chem.* 266:4862–4868.
Rijnboutt, S., W. Stoorvogel, H. J. Geuze, and G. J. Strous. 1992. Identification of subcellular compartments involved in biosynthetic processing of cathepsin D. *J. Biol. Chem.* 267:15665–15672.
Robinson, J. M., and M. J. Karnovsky. 1991. Rapid-freezing cytochemistry: preservation of tubular lysosomes and enzyme activity. *J. Histochem. Cytochem.* 39:787–792.
Robinson, M. S. 1994. The role of clathrin, adaptors and dynamin in endocytosis. *Curr. Opin. Cell Biol.* 6:538–544.
Rothman, J. E. 1994. Mechanisms of intracellular protein transport. *Nature (Lond.).* 372:55–63.
Ruscetti, T., J. A. Cardelli, M. L. Niswonger, and T. J. O'Halloran. 1994. Clathrin heavy chain functions in sorting and secretion of lysosomal enzymes in *Dictiostelium discoideum. J. Cell Biol.* 126:343–352.
Sandoval, I. V., and O. Bakke. 1994. Targeting of membrane proteins to endosomes and lysosomes. *Trends Cell Biol.* 4:292–297.
Schmid, S. L., and E. Smythe. 1991. Stage-specific assays for coated pit formation and coated vesicle budding in vitro. *J. Cell Biol.* 114:869–880.
Schonhorn, J. E., and M. Wessling-Resnick. 1994. Brefeldin A down-regulates the transferrin receptor in K562 cells. *Mol. Cell. Biochem.* 135:159–169.
Seaman, M. N. J., C. L. Ball, and M. S. Robinson. 1993. Targeting and mistargeting of plasma membrane adaptors in vitro. *J. Cell Biol.* 123:1093–1105.
Slot, J. W., H. J. Geuze, S. Gigengack, G. E. Lienhard, and D. E. James. 1991. Immuno-localization of the insulin regulatable glucose transporter in brown adipose tissue of the rat. *J. Cell Biol.* 113:123–135.
Stamnes, M. A., and J. E. Rothman. 1993. The binding of AP-1 clathrin adaptor particles to Golgi membranes requires ADP-ribosylation factor, a small GTP-binding protein. *Cell.* 73:999–1005.
Stoorvogel, W., H. J. Geuze, and G. J. Strous. 1987. Sorting of endocytosed transferrin and asialoglycoprotein occurs immediately after internalization in HepG2 cells. *J. Cell Biol.* 104:1261–1268.
Stoorvogel, W., H. J. Geuze, J. M. Griffith, and G. J. Strous. 1988. The pathways of endocytosed transferrin and secretory protein are connected in the *trans*-Golgi reticulum. *J. Cell Biol.* 106:1821–1829.
Stoorvogel, W., H. J. Geuze, J. M. Griffith, A. L. Schwartz, and G. J. Strous. 1989. Relations between the intracellular pathways of the receptors for transferrin, asialoglycoprotein, and mannose 6-phosphate in human hepatoma cells. *J. Cell Biol.* 108:2137–2148.
Stoorvogel, W., A. L. Schwartz, G. J. Strous, and R. J. Fallon. 1991*a*. A pool of intracellular phosphorylated asialoglycoprotein receptors which is not involved in endocytosis. *J. Biol. Chem.* 266:5438–5444.
Stoorvogel, W., G. J. Strous, H. J. Geuze, and A. L. Schwartz. 1991*b*. Late endosomes derive from early endosomes by maturation. *Cell.* 65:417–427.
Strous, G. J., P. van Kerkhof, G. van Meer, S. Rijnboutt, and W. Stoorvogel. 1993. Differential effects of brefeldin A on transport of secretory and lysosomal proteins. *J. Biol. Chem.* 268:2341–2347.
Tooze, J., and M. Hollinshead. 1991. Tubular early endosomal networks in AtT20 and other cells. *J. Cell Biol.* 115:635–653.
Traub, L. M., J. A. Ostrom, and S. Kornfeld. 1993. Biochemical dissection of AP-1 recruitment onto Golgi membranes. *J. Cell Biol.* 123:561–573.
Trowbridge, I. S., J. F. Collawn, and C. R. Hopkins. 1993. Signal-dependent membrane protein trafficking in the endocytic pathway. *Annu. Rev. Cell Biol.* 9:129–161.
Wang, L. H., K. G. Rothberg, and R. G. W. Anderson. 1993. Mis-assembly of clathrin lattices on endosomes reveals a regulatory switch for coated pit formation. *J. Cell Biol.* 123:1107–1117.
Wong, S. H., and W. Hong. 1993. The SXYQRL sequence in the cytoplasmic domain of TGN38 plays a major role in trans-Golgi network localization. *J. Biol. Chem.* 268:22853–22862.
Wood, S. A., J. E. Park, and W. J. Brown. 1991. Brefeldin A causes a microtubule-mediated fusion of the trans-Golgi network and early endosomes. *Cell.* 67:591–600.